Quantum description of a pseudointegrable system: The $\pi/3$-rhombus billiard

Debabrata Biswas and Sudhir R. Jain
Theoretical Physics Division, Central Complex, Bhabha Atomic Research Centre, Bombay 400 085, India
(Received 22 March 1990; revised manuscript received 1 June 1990)

The $\pi/3$-rhombus billiard is an example of the simplest pseudointegrable system having an invariant integral surface of genus $g=2$. We examine the fluctuation properties of eigenvalue sequences belonging to the "pure rhombus" modes (the eigenfunctions take nonzero values on the shorter diagonal). The nearest-neighbor spacing statistics follow the Berry-Robnik distribution with a chaotic fraction $\bar{\nu}$ (corresponding to the Liouville measure of the chaotic subspace) equal to 0.8. The spectral rigidity closely agrees with such a partitioning of phase space. The nodal patterns and the path correlation function exhibit irregularity for most of the corresponding eigenfunctions. Though the amplitude distributions for these closely approximate a Gaussian distribution, the spatial correlations do not agree well with the well-known Bessel oscillations. A few eigenfunctions, however, show regularity. These are localized in those regions of configuration space where the bouncing-ball modes form rectangular bands. The Born-Oppenheimer approximation offers a suitable explanation in terms of a confining potential, and the agreement between the exact and adiabatic eigenvalues improve at higher energies. On the basis of these observations, it turns out that the quantities ν and $\bar{\nu}$ are, in fact, the fractions of regular and irregular states in the eigenvalue sequence under consideration. Thus irregular eigenfunctions do occur for systems with zero Kolmogorov entropy, and the eigenvalue sequence corresponding to these yield Gaussian orthogonal ensemble statistics.

I. INTRODUCTION

The study of quantum eigenstates of classically nonintegrable Hamiltonian systems has elicited considerable interest in recent years.[1] Though their spectral properties have been understood reasonably well for some time, a general formalism has only now begun to emerge with the astounding success of the periodic orbit theory in explaining several properties of the eigenfunctions. Various routes have, however, led to the present status. Berry quantized the Sinai billiard[2] by converting the dynamical problem into one of band structure, which, in turn, was solved by the Korringa-Kohn-Rostoker procedure. Gutzwiller, on the other hand, developed the periodic theory[3] and realized its application successfully by quantizing the chaotic anisotropic Kepler problem.[4] This profound work illustrates the connection between classical periodic orbits and the eigenvalues of the quantum system. Yet again, McDonald[5] and McDonald and Kaufman,[6] using a numerical scheme developed by Riddell,[7,8] investigated various quantum signatures of the Bunimovich stadium billiard. It has indeed served as a useful model since for verifying several conjectures on mixing systems.

In the case of integrable systems, direct quantization schemes such as WKB or EBK give good approximations, at least in the large-k (small de Broglie wavelength) limit. Such methods are, however, ineffective when applied to classically nonintegrable systems and one has to take recourse to global quantization schemes such as the periodic orbit theory of Gutzwiller.[3] Problems in implementation arising from the difficulty in enumerating all the periodic orbits have limited its usage. Such orbits proliferate exponentially with increasing time periods in chaotic systems. Wintgen[9] has dealt successfully with the problem of a hydrogen atom in a uniform magnetic field and shown that if the summation is taken as an asymptotic series, contributions from longer orbits may be neglected. More recently, Aurich and Steiner[10] have studied the Hadamard-Gutzwiller model, which is a two-dimensional Hamiltonian system describing the geodesic flow on a surface of constant negative curvature. They have been able to classify and evaluate the lengths of the periodic orbits and apply them successfully to both the symmetric[11] and asymmetric models.[12]

Much of the current research until late has centered around the fluctuation properties of eigenvalue sequences. For generic integrable systems where the energy contours in action space are curved, Berry and Tabor[13] give strong arguments in support of a Poisson distributed spectrum. The numerical explorations of Bohigas, Giannoni, and Schmit,[14] on the other hand, led to the conjecture that the spectral fluctuations of time reversal invariant chaotic systems follow Gaussian orthogonal ensemble (GOE) statistics. Both the results have found credence in the semiclassical derivation of the spectral rigidity by Berry.[15] The transition from regular to chaotic motion has also been studied in detail[16–18] and the Berry-Robnik[19] distribution has proven to be a likely candidate for the level statistics.[20,21]

Though eigenfunctions contain much information, their nature and properties have remained largely unknown. For quasiperiodic dynamics, one can locally write the wave function as a sum over a finite number of plane waves in the short-wavelength limit. The summation is over the number of distinct ways in which a point

q can be accessed. However, if one extends the idea to chaotic motion, the wave function has to be expressed as a sum over an infinite number of plane waves, each having a random amplitude, phase, and direction. This leads to a Gaussian amplitude distribution and a spatial correlation function with Bessel function dependence. For the Bunimovich stadium billiard, which is a mixing system with an exponential divergence of trajectories, most ($\approx 90\%$) of the eigenstates corroborate these assertions. However, there exist eigenfunctions both at low[22] and high[23] energies which behave otherwise. Most of these are localized on families of regular trajectories with short periods, while others have a large amplitude on a single unstable periodic orbit. Using the Born-Oppenheimer approximation, Bai *et al.*[24] have been able to show that a dynamical confining potential can indeed be constructed to explain the localization effect in the former case. The latter phenomenon, popularly known as "scarring," was first observed by Heller.[25] A considerable body of knowledge has evolved since out of the works of Bogomolny[26] and Berry,[27] and it is now well established that as in case of eigenvalues, periodic orbits influence individual eigenfunctions as well. Thus quantum manifestations of classical dynamics show up as "scars" on wave functions. Other reasons for the keen interest in the properties of eigenfunctions stem from a desire to extend the well-developed semiclassical methods of quasiperiodic dynamics to chaotic systems.

The characterization of regular and irregular states has, of course, been a major research topic since it has severe implications for chemists, spectroscopists, plasma physicists, and many others—for different reasons though. Regular dynamics in classically nonintegrable systems gives rise to the concept of local actions and leads to trajectories that are confined to tori. The mechanism, however, is not obvious. Quantum mechanically, the corresponding states can now be labeled by locally good quantum numbers. The eigenfunctions in most cases (certainly those at higher energies) are localized and have regular nodal pattern in the region of confinement. Thus, over the years, regular and localized states have come to mean the same thing.

While integrable and chaotic systems represent two extreme behaviors, pseudointegrable systems fall in a category in between. Polygonal billiards with at least one angle in the form $m\pi/n$ ($m \neq 1$) fall under this category. In a sense, these are the nearest step away from integrability since their invariant integral surface has a genus greater than one (for a torus, $g=1$) despite the existence of two integrals of motion. This happens because the integrals are in involution everywhere except at the vertices. As a result, one of the assumptions of the Liouville-Arnold theorem stands violated. Zemlyakov and Katok[28] were the first to study these systems, while Richens and Berry[29] were the first to quantize an example of this class. Their[29] results on the nearest-neighbor level spacing distribution show a linear level repulsion. Recently, Cheon and Cohen[30] have studied the spectral statistics of a series of pseudointegrable systems which approximate the Sinai billiard increasingly well (essentially going to surfaces of higher genus). The agreement with the predictions of GOE improves as the approximation gets better. However, since they have confined themselves to the low-energy regime, the authors indicate that these results reflect a purely quantum phenomenon, thereby implying that a transition in the spectral statistics could occur at higher energies. Seba,[31] however, argues that since the relevant scale is represented by the edges of the corners, which in fact are point objects, the semiclassical regime should set in only at $E \to \infty$. Thus GOE statistics should prevail at all energies. The point is substantiated by his study of a singular billiard system[31] where the level statistics is seen to coincide with the predictions of GOE.

To the best of the authors' knowledge, there has been no explicit study on the wave functions of pseudointegrable systems. Richens and Berry[29] conjectured that those eigenfunctions of the $\pi/3$-rhombus billiard which do not vanish on the shorter diagonal have contributions from an infinite number of evanescent waves. No concrete evidence exists however. It is important, therefore, to understand the manifestations of pseudointegrability on both the spectrum and the eigenfunctions and to try to relate the two.

In the following sections, we shall discuss the $\pi/3$-rhombus billiard (Fig. 1), which is known[29,32] to be a pseudointegrable system having a classically invariant surface of genus $g=2$. A full quantum description of such a system does not exist analytically as yet. It is easy to see, however, that half the eigensolutions are identical to those of an equilateral triangle, which is an integrable though nonseparable system. In fact, a semiclassical analysis using the Keller-Rubinow[33] ansatz yields only these solutions. The other half (equivalent to an equilateral triangle with one Neumann and two Dirichlet edges) would no doubt help us to understand the implications of nonintegrability in the quantum system. A few low-lying states of these have been obtained by Gaudin.[34]

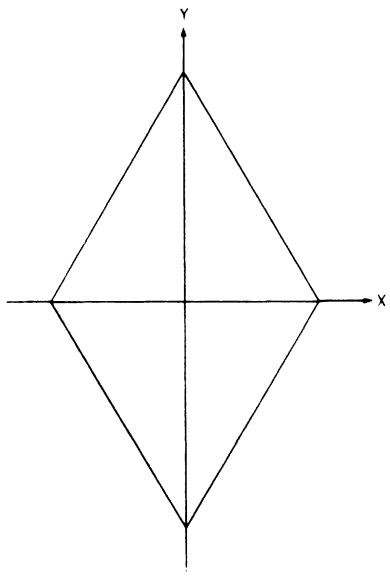

FIG. 1. The $\pi/3$-rhombus billiard. The particle reflects specularly from the walls.

The plan of the paper is as follows. Section II contains a study of the spectral fluctuations of the "pure" rhombus modes. In Sec. III we apply various diagnostic techniques to determine the nature of these eigenfunctions. Numerical evidence of the existence of localized states is also provided and a comparative study with the equilateral triangle eigenfunctions is made to facilitate interpretation. The localization phenomenon is suitably explained in terms of the Born-Oppenheimer approximation in Sec. IV. In Sec. V we apply these results to interpret the observations on the spectral statistics discussed in Sec. II. Finally, we summarize our results in Sec. VI. For all quantitative results in this paper $\hbar^2/2m=1$ and the sidelength L of the rhombus is $2\pi/3$.

II. EIGENVALUES AND SPECTRAL STATISTICS

In this section we present our results on the nearest-neighbor level distribution (NNLD) and the spectral rigidity $\bar{\Delta}_3$. In order to isolate the effects of the equilateral triangle eigenstates on the spectral fluctuations, we have considered only the "pure" rhombus modes.

The eigenvalues have been obtained by employing the boundary dipole distribution technique discussed in the Appendix. The first few levels of the equilateral triangle are listed in Table I along with the exact ones obtained analytically. These have a mean relative accuracy of $\sim 10^{-6}$. The statistical tests discussed in this section deal with the eigenvalues in the interval $25<k<70$. The mean relative accuracy of the equilateral triangle eigenvalues in this region is $\sim 10^{-4}$. We assume the same to hold for the pure rhombus modes. For the sake of comparison, we present in Table II the values obtained by Gaudin.[34]

A consequence of classical nonintegrability is that individual levels are hard to determine semiclassically. The exact nature of nonintegrability is also reflected in the statistical properties of sequences of many levels. Thus time-reversal invariant chaotic systems follow GOE statistics,[14,15] while those which do not possess this symmetry follow Gaussian unitary ensemble (GUE) statistics.[15,35] On the other hand, the large number of almost degenerate eigenvalues in generic integrable systems leads to a Poisson level statistics.

TABLE I. Numerically obtained eigenvalues E_1 along with the exact ones E_2 of the equilateral triangle. The mean relative error is $\sim 0.000\,001$.

E_1	E_2
12.000 001	12
28.000 006	28
48.000 050	48
52.000 089	52
76.000 121	76
84.000 195	84
108.000 030	108
112.000 253	112
123.999 723	124
148.000 410	148
156.000 337	156
192.000 057	192
196.000 543	196

TABLE II. A few low-lying states of the "pure" rhombus modes. E_1 is the value obtained using the boundary integration technique, while E_2 is that computed by Gaudin (Ref. 34). The sidelength of the rhombus is $2\pi/\sqrt{3}$.

E_1	E_2
1.890 970	1.892
6.369 447	6.370
10.665 749	10.673
12.859 805	12.854
26.781 918	26.80
34.256 016	34.25

The integrated density of states $N(E)$ of a quantum system consists of two terms. Superimposed on the average smooth part is the nonanalytic fluctuating part. Thus

$$N(E)=N_{\rm av}(E)+N_{\rm fl}(E)\ . \tag{2.1}$$

The first step in an analysis of spectral fluctuations is to eliminate the average trend. This procedure, known as "unfolding," is particularly simple in the case of billiard systems where one can use the Weyl formula[36]

$$N(E)=AE/4\pi+\sqrt{E}\,(L_n-L_d)/4\pi+C+D\ , \tag{2.2}$$

where A is the area, and L_n and L_d are the lengths of Neumann and Dirichlet edges. The quantities C and D are corrections due to vertices and curvature. For polygonal billiards, the latter term is zero.

A sequence $\{\varepsilon_i\}$ with the mean spacing unity can thus be generated using the mapping $\varepsilon_i=N_{\rm av}(E_i)$. The simplest statistical measure of this new sequence is the nearest-neighbor spacing distribution $P(s)$. It is defined such that $P(s)ds$ is the probability of finding adjacent pairs $(j,j+1)$ with a spacing $\varepsilon_{j+1}-\varepsilon_j$ lying between s and $s+ds$.

Berry and Tabor[13] give strong arguments to show that in generic integrable systems, where the energy contours in action space are curved, the levels are indeed uncorrelated and the spacing distribution $P(s)$ is given by

$$P(s)=\exp(-s)\ , \tag{2.3}$$

characteristic of a Poisson process. The nonzero value of $P(s)$ in the limit $s\to 0$ is referred to as level clustering. It is well known, however, that certain systems violate the above-mentioned correspondence. The simplest example is a square billiard. The difference in behavior is attributed to the fact that the classical orbits picked by imposing the quantum conditions are all closed, indicating that the system under consideration is "nongeneric."[13] Shudo[37] has, however, shown that the NNLD's of integrable systems do exhibit a system-specific behavior.

On the other hand, time-reversal invariant chaotic systems are characterized by level repulsion. The spacing distribution is seen to follow the Wigner distribution[12,14]

$$P(s)=(\pi s/2)\exp[-(\pi/4)s^2]\ , \tag{2.4}$$

a result, known to be true for complex systems having many degrees of freedom.

For an N-dimensional generic system, however, the phase space is mixed. Some orbits reside on an N-dimensional torus while others explore the entire $(2N-1)$-dimensional region chaotically. Berry and Robnik[19] suggest that the spectral fluctuations should result from independently superposing a Poisson spectrum with a relative weight ν and a series of GOE spectra corresponding to disconnected chaotic regions of phase space with relative weights ν_i such that $\nu+\sum_i \nu_i=1$. In the simplest case of a single chaotic region (for $N\geq 3$, Arnold diffusion ensures the existence of a single chaotic subspace),

$$P(s)=\nu^2\exp(-\nu s)\operatorname{erfc}(\sqrt{\pi}\bar{\nu}s/2) + (2\nu\bar{\nu}+\pi\bar{\nu}^3 s/2)\exp(-\nu s-\pi\bar{\nu}^2 s^2/4) . \quad (2.5)$$

Higher-order correlations contain more information. Among the useful ones is the spectral rigidity $\bar{\Delta}_3$ of Dyson and Mehta.[38] It measures the mean-square deviation of the integrated density of states from a straight line in an interval $[x-L/2,x+L/2]$. It is defined as

$$\bar{\Delta}_3(L)=\left\langle \min_{A,B}\frac{1}{L}\int_{-L/2}^{L/2} d\varepsilon[N(x+\varepsilon)-A-B\varepsilon]^2 \right\rangle . \quad (2.6)$$

One can eliminate the constants A and B to obtain

$$\bar{\Delta}_3(L)=\left\langle \frac{1}{L}\int_{-L/2}^{L/2} d\varepsilon\, N^2(x+\varepsilon) - \left[\frac{1}{L}\int_{-L/2}^{L/2} d\varepsilon\, N(x+\varepsilon)\right]^2 - 12\left[\frac{1}{L^2}\int_{-L/2}^{L/2} d\varepsilon\,\varepsilon N(x+\varepsilon)\right]^2 \right\rangle . \quad (2.7)$$

Using the semiclassical form for the fluctuating part of the density of states $d_{\rm osc}$, Berry[15] has shown that for generic integrable systems,

$$\bar{\Delta}_3(L)=L/15 \quad \text{for } L\ll L_{\max} , \quad (2.8)$$

while for $L\gg L_{\max}$, $\bar{\Delta}_3(L)$ saturates nonuniversally, where $L_{\max}=h\langle d\rangle/T_{\min}$, $T_{\min}$ being the period of the shortest classical orbit. The averaging in Eq. (2.6) is over an energy interval much larger than $L_{\max}$, but still classically small.

For time-reversal invariant chaotic systems with isolated unstable periodic orbits, the spectral rigidity takes the form[15]

$$\bar{\Delta}_3(L)\approx \ln(L)/\pi^2-0.00695 \quad \text{for } L\ll L_{\max} , \quad (2.9)$$

while it saturates nonuniversally for $L\gg L_{\max}$.

Before we proceed with our results on level correlations, we wish to emphasize that any statistical tests of this nature are meaningful only if the mode number satisfies the Weyl asymptotic formula. We have plotted the staircase function $N(E)$ in the interval $25<k<70$ [Figs. 2(a) and 2(b)] and compared them with the Weyl result of Eq. (2.2). The quantity C in this case is $\frac{5}{12}$.

The solutions of the Schrödinger equation can be classified into four different parity modes (Fig. 1):

$$\psi(x,y)=\begin{cases}\psi(-x,y)=\psi(x,-y), & (00)\text{ parity mode}\\ \psi(-x,y)=-\psi(x,-y), & (01)\text{ parity mode}\\ -\psi(-x,y)=\psi(x,-y), & (10)\text{ parity mode}\\ -\psi(-x,y)=-\psi(x,-y), & (11)\text{ parity mode.}\end{cases} \quad (2.10)$$

The wave functions corresponding to the (00) and (10) parity modes do not vanish on the shorter diagonal. We refer to these as the "pure rhombus" modes. On the other hand, the (01) and (11) modes are identical to those of the equilateral triangle.

Figures 3(a) and 4(a) show the nearest-neighbor level

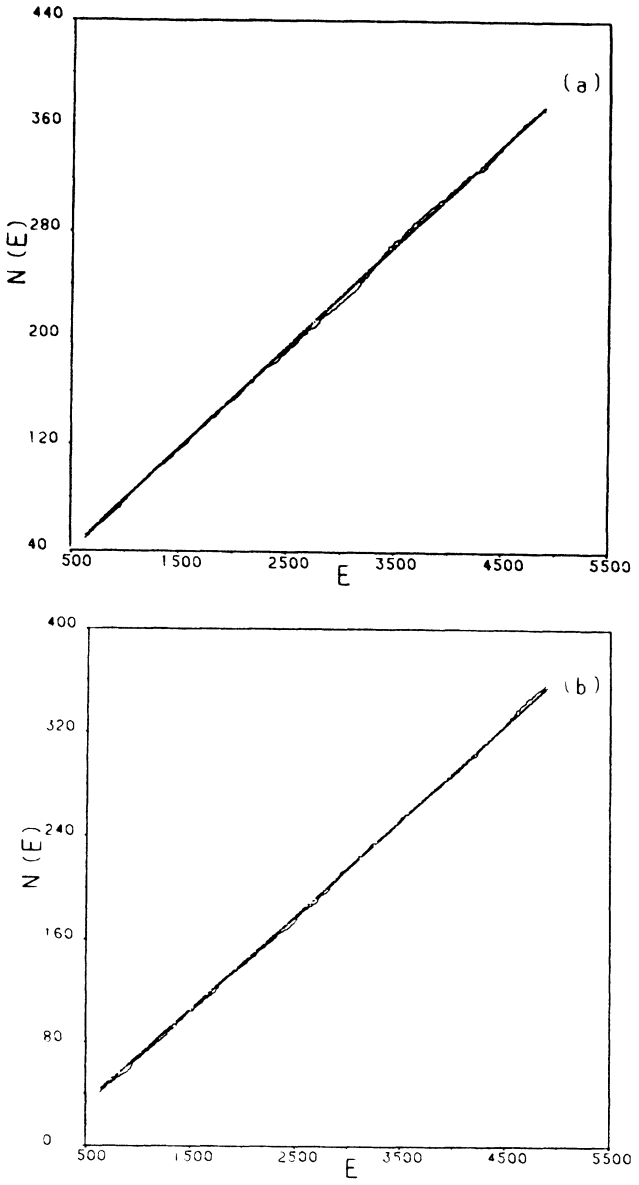

FIG. 2. Integrated density of states $N(E)$ for the (a) (00) and (b) (10) parity modes. The dotted curve denotes the corrected Weyl result given by Eq. (2.2).

spacing statistics of the pure rhombus modes. The continuous curve in both cases is the Berry-Robnik distributioln with $\bar{\nu}=0.8$. Considering the fact that the system at hand has a zero Kolmogorov entropy (Lyapunov exponents are zero), the result certainly is surprising. It would be more appropriate to introduce the quantities $\bar{\nu}_{cl}$, calculated by studying the classical motion and $\bar{\nu}_{qm}$ obtained from the best fit to the spacing distribution. Comparisons between the two have been made previously by Zimmermann *et al.*[20] for various systems and probable explanations for the deviation have also been given.

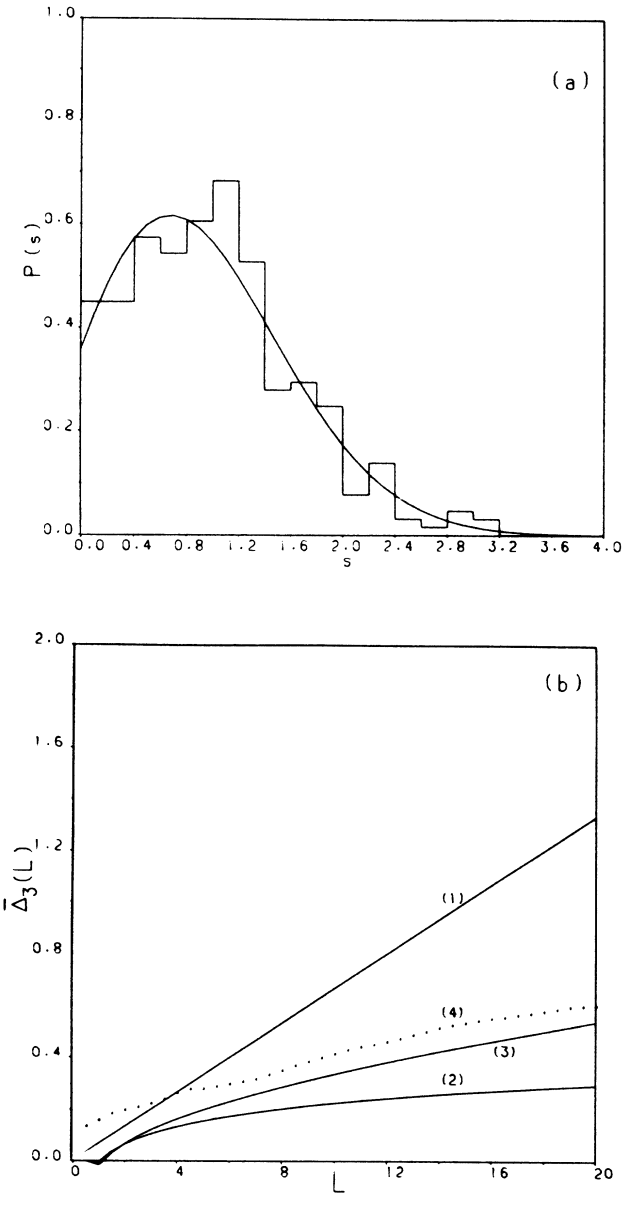

FIG. 3. Spectral statistics of the (00) parity mode: (a) shows the nearest-neighbor level-spacing distribution. The continuous curve denotes the Berry-Robnik distribution with $\nu=0.2$. (b) shows the spectral rigidity $\bar{\Delta}_3(L)$. Curve 4 (dotted) is the numerical result while 1 and 2 are those for the integrable and chaotic cases, respectively. Curve 3 follows Eq. (2.11) with $\nu=0.2$.

The worst case corresponds to $\bar{\nu}_{cl}=0$ and $\bar{\nu}_{qm}=0.4$, and in general the difference is large for small values of $\bar{\nu}_{cl}$. The anomaly has been attributed to the slow convergence to the semiclassical limit for nearly integrable systems. The same does not hold for pseudointegrable systems though. Besides, a drastic change in the level statistics at higher energies seems unlikely. The result of Richens and Berry[29] also supports this fact. This would seem to suggest that an exponential divergence of trajectories is not a necessary condition for a GOE-like spectrum.

The $\bar{\Delta}_3$ statistic of the (00) and (10) modes are shown in Figs. 3(b) and 4(b). The straight line in both cases corresponds to the integrable result, while curve 2 is given by Eq. (2.9). The numerical results in both cases fall between the two limiting cases. Visual inspection, however, indicates that it lies close to the GOE result.

The partitioning of the phase space leads to a result

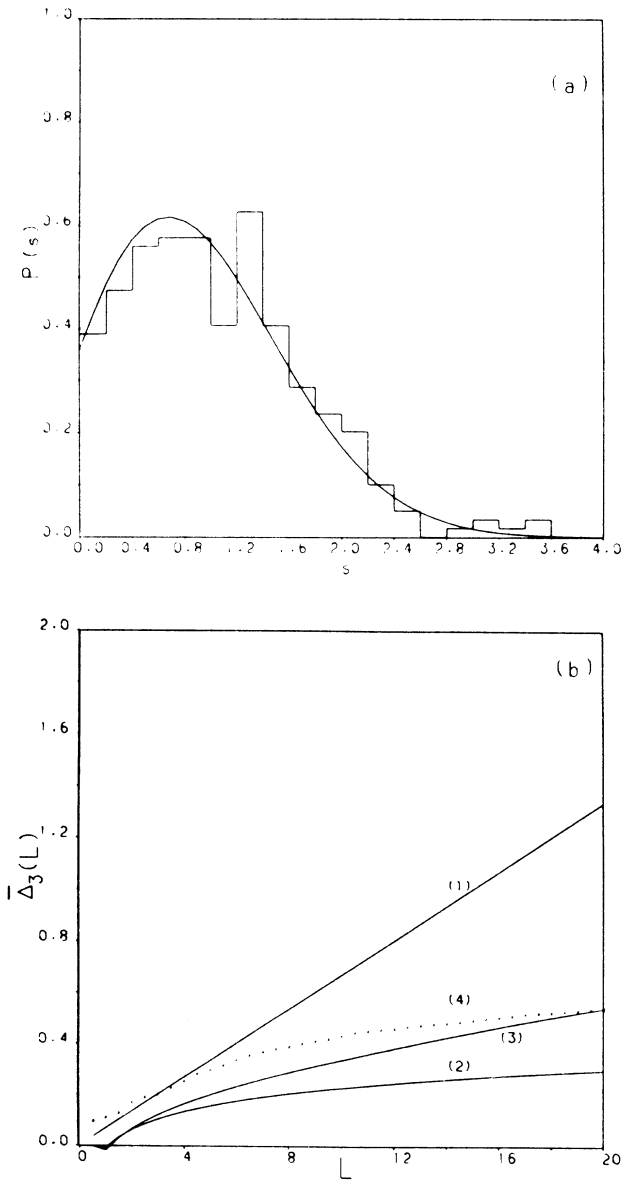

FIG. 4. Same as in Fig. 3 for the (10) parity mode.

analogous to the Berry-Robnik distribution for the $\bar{\Delta}_3$ statistic.[39] Using the same notation,

$$\bar{\Delta}_3(L)=\Delta_3^{\mathrm{Poi}}(\nu L)+\sum_i \Delta_3^{\mathrm{GOE}}(\bar{\nu}_i L) , \tag{2.11}$$

where $\nu+\sum_i \bar{\nu}_i=1$, and the index Poi represents Poisson.

Curve 3 shows Eq. (2.11) with a single chaotic volume $\bar{\nu}=0.8$ as in the Berry-Robnik distribution. The agreement with the numerical result is fair and improves for large L.

Thus even when the classical flow is restricted to a double torus, the statistical properties of the eigenvalues resemble those of random matrices belonging to the Gaussian orthogonal ensemble. We provide further support for these assertions in Sec. V.

III. EIGENFUNCTIONS AND THEIR PROPERTIES

The analysis of the spectral fluctuations clearly indicates that there exists a close analogy in the quantum description of our system with typical chaotic billiards. Is it, however, restricted to the spectral properties alone or does it show up in the eigenfunctions as well? Are typical eigenstates belonging to the (00) and (10) parity modes irregular? We seek to investigate these questions in the following subsections.

The eigenfunctions have been obtained using the boundary dipole distribution technique (see the Appendix). For the statistical tests discussed in Secs. III B and III C a total of 9641 points have been taken in the first quadrant of the rhombus. In order to have a meaningful comparison between the equilateral triangle and pure rhombus modes, all eigenfunctions have been normalized to unity.

A. Nodal patterns

Nodal curves give the standing-wave pattern on vibrating membranes and were studied extensively in theoretical acoustics. They have also found wide applicability in quantum mechanics. Pechukas[40] attempted to generalize the Miller-Good transformations in more than one dimension in an endeavor to obtain nodal coordinates which form a separable system for individual eigenfunctions, an idea which was studied extensively by DeLeon and Heller[41] later. It has also been widely used to distinguish regular and irregular waves.[5]

Heller[25] has, however, shown that an irregular-looking nodal plot is not sufficient for quantum mechanics to "mimic" classical chaos. The latter implies an infinite number of directions, while a superposition of even six cosine waves with random direction and phase but equal wave-vector magnitude is sufficient to generate a complex nodal pattern.

The equilateral triangle wave functions result from a superposition of six plane waves with equal wave-vector magnitude, but directions that are far from random. They are related to each other by the laws of reflection. In Fig. 5(a), we present the nodal pattern of a typical triangle eigenfunction at an intermediate energy. The regularity is rather evident. On the other hand, the nodal plot of a neighboring (00)-mode eigenfunction [Fig. 5(b)]

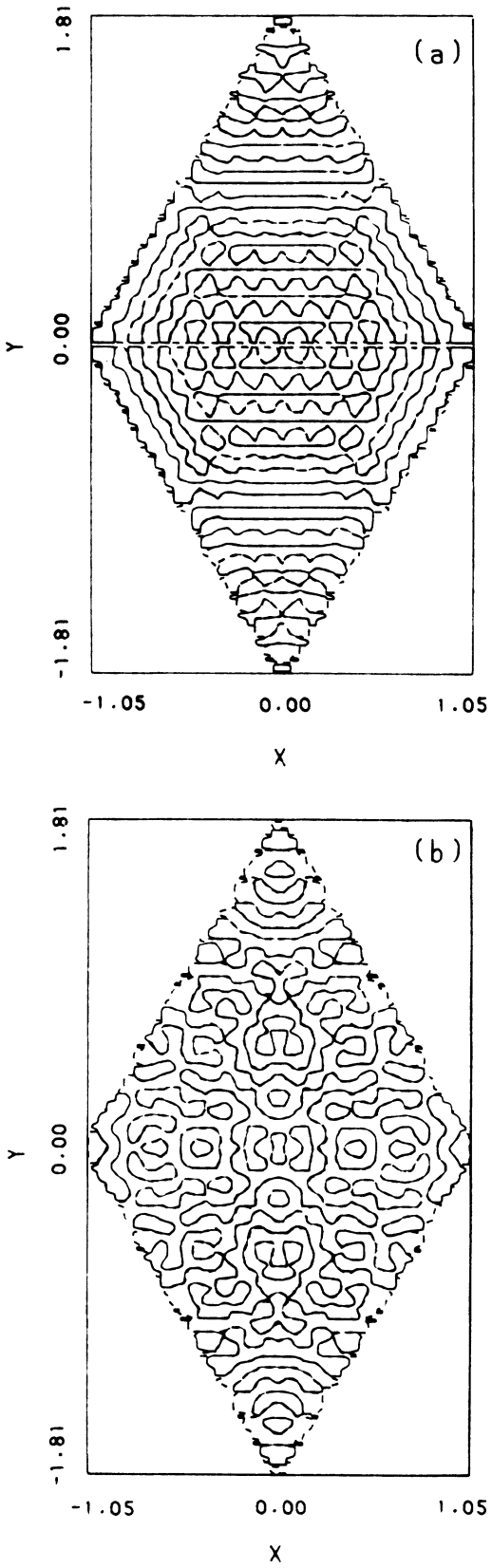

FIG. 5. Nodal plot for (a) the (01) parity mode eigenfunction at $k=45.0776$ and (b) the (00) parity mode eigenfunction at 45.0298. The regular-looking patterns in the former case are in sharp contrast to the irregular curves for the "pure" rhombus eigenfunction.

shows considerable irregularity and many more avoided crossings. At higher energies these patterns become rather complicated and it is difficult to make out the difference unless magnified.

While most of the (00)-mode eigenfunctions behave in a similar fashion, some of them do exhibit regularity. These take appreciable nonzero value in the two bands shown in Fig. 6 and are nearly zero in the rest of the domain. Figure 7 shows a contour plot of a typical localized eigenfunction at $k=64.1408$ belonging to the (00) parity mode. Its nodal curve (Fig. 8) shows considerable regularity in the region of localization and is distinctly different from the complex patterns of the neighboring (00) parity eigenfunctions.

Thus nodal patterns indeed serve as a criterion to distinguish a regular wave from an irregular one. It is, however, not possible to identify the number of randomly superposed plane waves. We hope to make these observations more concrete in the following subsections.

B. Amplitude distribution $P(\psi)$

In chaotic billiard systems, the description of the wave function is based on the concept of eikonal theory, according to which the eigenfunction ψ can be locally represented by a superposition of an infinite number of plane waves with equal wave-vector magnitude but random phases and directions. By the central limit theorem then, $\psi(x)$ is a Gaussian random variable. It is well known that a superposition of a few random variables with identical distributions is sufficient to give a good approximation to a Gaussian distribution. Thus once more, the very fact that the amplitude distribution for a particular wave function is Gaussian is not sufficient to infer that the corresponding classical system is chaotic. The test, however, can be used to distinguish regular and irregular waves and it is possible to quantify the degree of irregularity as we shall see. In the following, we present our investigations in several energy ranges. As before, we

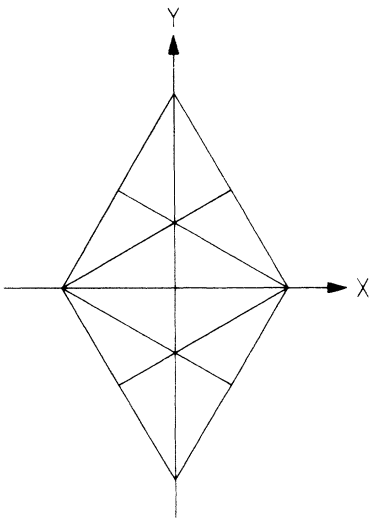

FIG. 6. The $\pi/3$-rhombus billiard along with the two rectangular bands in which the regular eigenfunctions belonging to the (00) parity mode are localized.

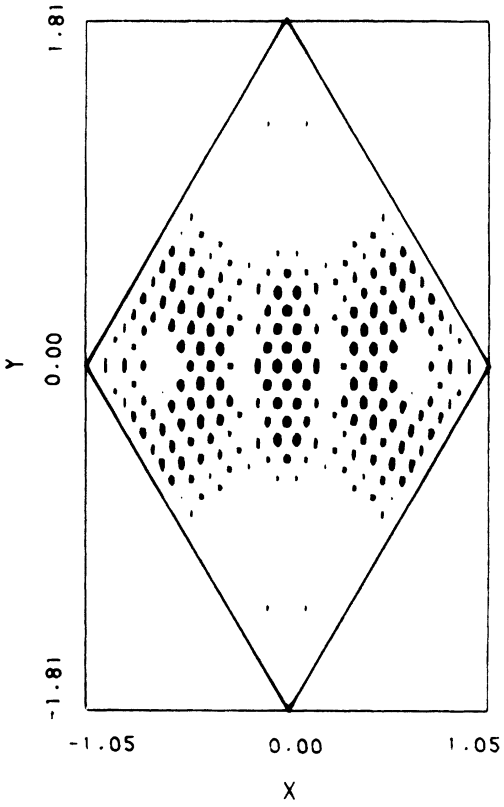

FIG. 7. Contour plot of the (00) parity mode eigenfunction at $k=64.1408$. The wave function is predominantly localized in the two bands shown in Fig. 6.

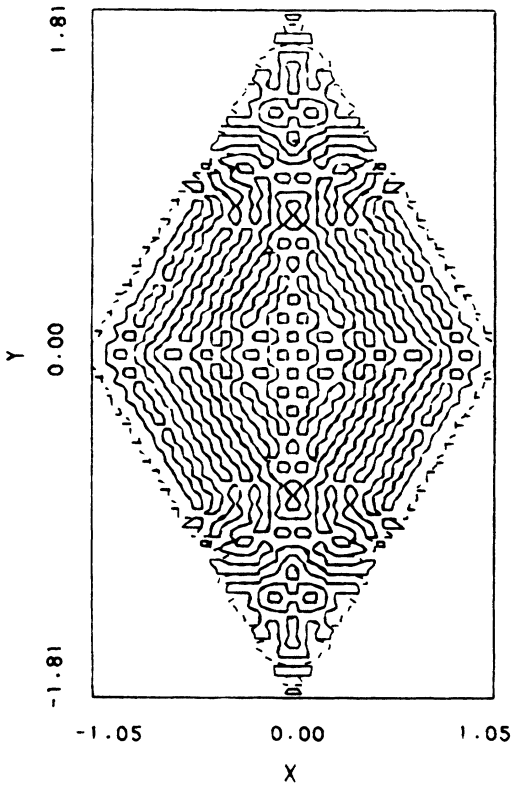

FIG. 8. The nodal plot corresponding to the localized eigenfunction ($k=64.1408$) shows considerable regularity in the region of confinement.

shall compare neighboring equilateral triangle and pure rhombus modes.

A total of 120 bins have been chosen in each case. Since the wave function and amplitude distribution have been normalized to unity, it is possible to define a goodness-of-fit parameter G as the mean-square deviation of $P(\psi)$ from the fitted Gaussian distribution. We have listed a few values in Table III.

Though the equilateral triangle eigenfunctions are comprised of six plane waves, they cannot be treated as independent random variables as we have remarked earlier. The amplitude distribution should, therefore, show considerable deviation from the Gaussian distribution. The values listed in Table III and Fig. 9(a) attest to this fact.

Clearly, at low energies the test is not good enough since we are far from the semiclassical limit. At higher energies, most of the (00) parity-mode eigenfunctions show a much better fit to a Gaussian distribution. A typical case is shown in Fig. 9(b) where $P(\psi)$ approximates a Gaussian distribution rather well.

For the localized eigenfunctions belonging to the (00) parity mode, the test naturally yields a different result. Figure 9(c) shows $P(\psi)$ for the eigenfunction at $k=64.1408$ considered earlier. The deviation is quite large and the value of G (Table IV) is comparable to those obtained for the equilateral eigenfunctions. This is in conformity with the observations of Sec. III A. We list a few values of the goodness-of-fit parameter G in Table IV for localized states occurring at various energies. It is interesting to note that the amplitude distributions for these localized eigenfunctions are similar to those of the bouncing ball modes in the stadium billiard.

Thus most eigenfunctions of the pure rhombus modes result from a superposition of a few independent sets of plane waves giving rise to a Gaussian amplitude distribution. The localized states, on the other hand, show considerable deviation and, moreover, behave in a manner identical to that of the equilateral triangle eigenfunctions.

C. Path correlation function (PCF)

Shapiro and Goelman,[42] using the intuitive equivalence of chaos with randomness, identified "fully developed chaos" in a quantum eigenstate with the path correlation function

$$F_n[\psi]=N^{-1}\sum_{i=1}^{N}\psi(r_i)\psi(r_{i+n}),\quad n<N \tag{3.1}$$

randomly fluctuating about zero for all $n>0$. Here N is the total number of points in the interior of the domain and the points r_i are ordered in a cyclic manner ($r_j=r_{j+n}$) on a space-filling self-avoiding path.

In the present case, $N=9641$ and $0\le n\le 1600$. The function $F_n[\psi]$ has been evaluated for two distinct paths, both of which are special to the system. Path 1 consists of straight segments that are parallel to the x axis, while path 2 consists of segments that are parallel to the y axis. It should be borne in mind that there exist families of periodic orbits that are parallel to both the diagonals.

TABLE III. Comparison of the goodness-of-fit parameter G for the the equilateral triangle and "pure" rhombus modes. The subscripts refer to the parities of the eigenfunctions. The fit to a Gaussian distribution is much better in case of the (00) parity mode.

k	G_{00}	G_{01}
22.5113	0.187	
22.5389		0.172
45.0298	0.045	
45.0776		0.193
48.1224	0.060	
48.1248		0.182
58.2186	0.090	
58.2065		0.970
65.7698	0.033	
65.5744		0.242

The test has nevertheless come under severe criticism since it depends on an arbitrary path through the system. We shall see that the behavior of most eigenfunctions belonging to the (00) parity mode is independent of the path chosen. Those where it does depend turn out to be the ones that are regular.

Figures 10(a) and 10(b) show the results of our investigations of a low-energy eigenfunction belonging to the (01) parity mode. The oscillations about zero for path 1 are weak and they possess a definite structure indicating a strong correlation. Path 2, however, shows quite a different behavior. On the other hand, for the neighboring (00) parity-mode eigenfunction, the oscillations are much more rapid and random for both the paths [Figs. 11(a) and 11(b)]. A similar behavior persists at higher energies for all eigenfunctions having a Gaussian amplitude distribution and irregular nodal patterns.

We present the results of our investigations of the localized eigenfunction belonging to the (00) parity mode at $k=64.1408$ in Fig. 12. For path 1 [Fig. 12(a)] the PCF possesses a definite structure and shows strong correlation while for the second path [Fig. 12(b)], the oscillations are much more rapid and random. The behavior is qualitatively similar to that of the equilateral triangle eigenfunctions.

Thus, while in case of most (00 parity mode eigenfunctions the PCF shows an uncorrelated random behavior for both the paths considered, the equilateral triangle and the localized eigenfunctions belonging to the (00) parity mode have patches of strong correlation for at least one of the paths. The test is effective at low energies also.

TABLE IV. Goodness-of-fit parameter G_{00} for a few localized eigenstates of the $\pi/3$-rhombus billiard. The values are comparable to those of the equilateral triangle modes.

k_{00}	G_{00}
51.9651	0.4389
57.2331	0.1732
64.1408	0.3652
78.0142	0.4839

D. Spatial correlation function

For an eigenfunction comprising of an infinite number of plane waves, Berry[43] showed that the spatial correlation function

$$C(\mathbf{s})=\int_A \psi^*(\mathbf{x}-\mathbf{s}/2)\psi^* \times(\mathbf{x}+\mathbf{s}/2)d\mathbf{x}\Big/\int_A \psi^*(\mathbf{x})\psi(\mathbf{x})d\mathbf{x} \qquad (3.2)$$

shows Bessel function oscillations that are independent of the direction of increment $\mathbf{s}$. Thus $C(\mathbf{s})=J_0(ks)$, where J_0 is the Bessel function of zero order, k and s being the magnitudes of $\mathbf{k}$ and $\mathbf{s}$, respectively. The integration is over all points $\mathbf{x}$ such that $\mathbf{x}+\mathbf{s}/2$ and $\mathbf{x}-\mathbf{s}/2$ lie in the interior of the domain. Naturally, one would not expect the pure rhombus eigenfunctions to behave in such a manner since the number of possible directions is finite.

The numerically computed spatial correlation function $C(s)$ is displayed in Fig. 13 for the (00) parity mode eigenfunction at $k=65.7698$. We have considered several directions for the increment $\mathbf{s}$ at random, but only two of these are shown in the figures. The fit to the Bessel function $J_0(ks)$ is good for small values of s, but shows considerable deviation after the first node. The same holds for all the other angles considered.

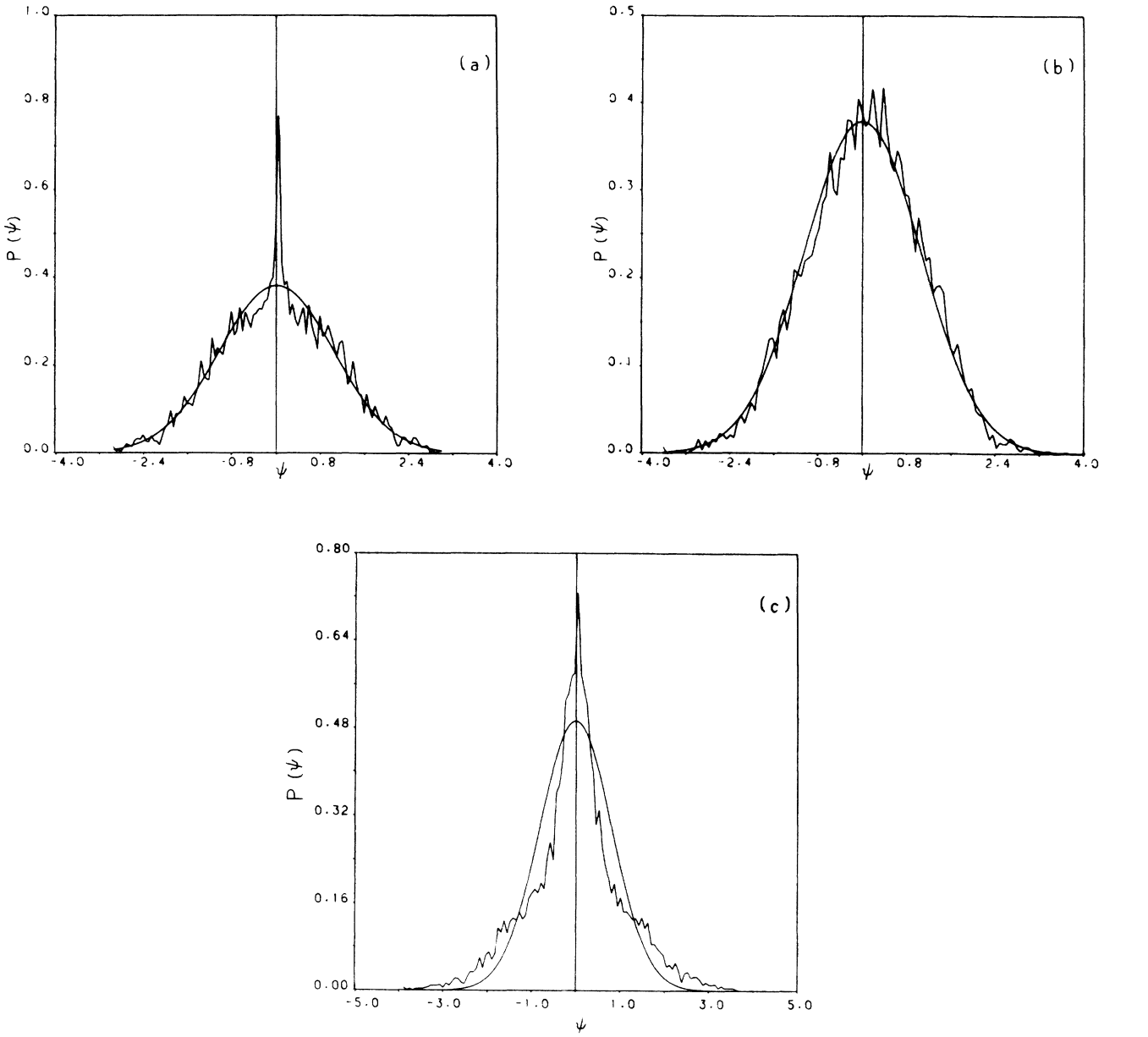

FIG. 9. Amplitude distribution $P(\psi)$ for (a) the (01) mode eigenfunction at $k=65.5744$, (b) the (00) mode eigenfunction at $k=65.7699$, and (c) the localized eigenfunction belonging to the (00) parity mode at $k=64.1408$. The fit to a Gaussian distribution is good in case (b), while the deviations are considerable for (a) and (c).

The triangle eigenfunctions behave similarly for small s, but the deviations get much more pronounced [than in the (00) parity case] thereafter. A typical example is shown in Fig. 14.

The lack of isotropy and the deviations from the Bessel function oscillations is much more evident for the localized eigenfunctions. Figure 15 illustrates the point. The oscillations, in fact, have a sinusoidal behavior.

Such investigations have been carried out for several other eigenvalues and the results turn out to be the same qualitatively. Similar studies have been done for the stadium billiard, which is a chaotic system.[5,6] While the agreement with the theoretical prediction was not perfect, the deviations were not as significant. In the present case, one can infer that the irregular pure rhombus eigenfunctions result from a random superposition of only a finite number of plane waves.

IV. LOCALIZED STATES FROM THE BORN-OPPENHEIMER APPROXIMATION

The Born-Oppenheimer approximation (BOA) has met with considerable success in explaining the presence of

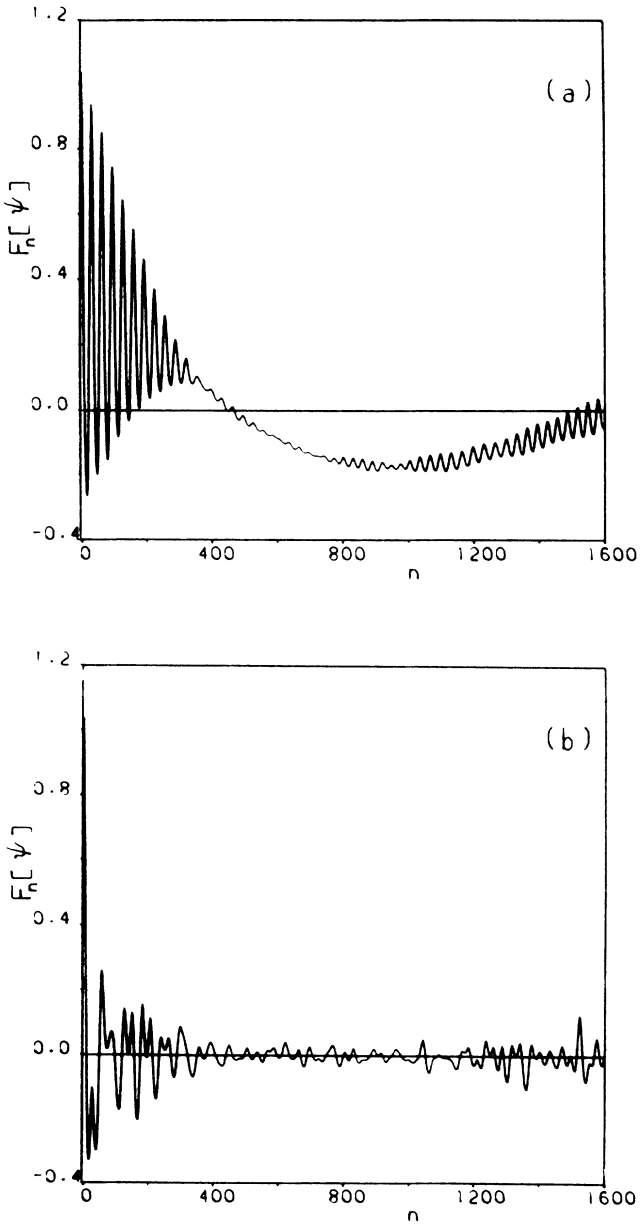

FIG. 10. Path correlation function $F_n[\psi]$ for the (01) parity mode eigenfunction at $k=22.5389$ along (a) path 1 and (b) along path 2.

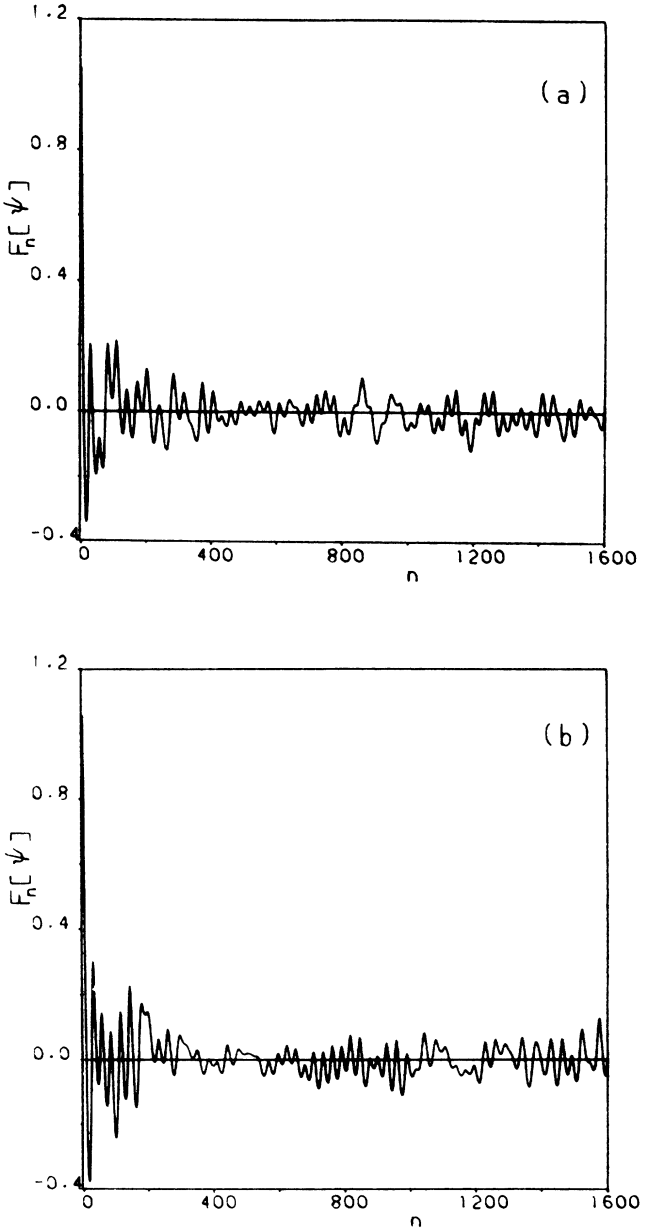

FIG. 11. Same as in Fig. 10 for the (00) parity mode eigenfunction at $k=22.5113$. The lack of correlation in both cases indicates the irregular nature of the eigenfunction. The test can be effectively used to distinguish regular and irregular states at low energies.

regular states in the mixing stadium billiard. The first attempts in this direction were made by Shapiro, Taylor, and Brumer.[22] Using the adibatic approximation, they were able to show that a few of the low-lying states are indeed regular. Later workers[24] were able to explain the existence of localized states at higher energies with the help of a confining potential which occurs quite naturally in the BOA. The theory, however, can be applied only when a band of periodic orbits exist, and hence fails to explain the occurrence of eigenfunctions localized on a single unstable periodic orbit (such as the "whispering gallery" modes in the stadium) in terms of a confining mechanism. As in all other polygonal billiards, periodic orbits in the $\pi/3$ rhombus billiard occur in bands and hence, the theory is best suited to investigate the presence of localized states in such a system. The choice of the coordinates is extremely important as pointed by Stefanski and Taylor.[44] For each quasiperiodic motion appearing in a system, a different separation is required which in general would be quite nontrivial. One must either know the trajectories or the wave functions explicitly. In the latter case, the idea of Pechukas[40] which was developed considerably by DeLeon and Heller[41] leads us to the nodal coordinates in which the separation can be carried out.

In this particular case, there exist bands of self-

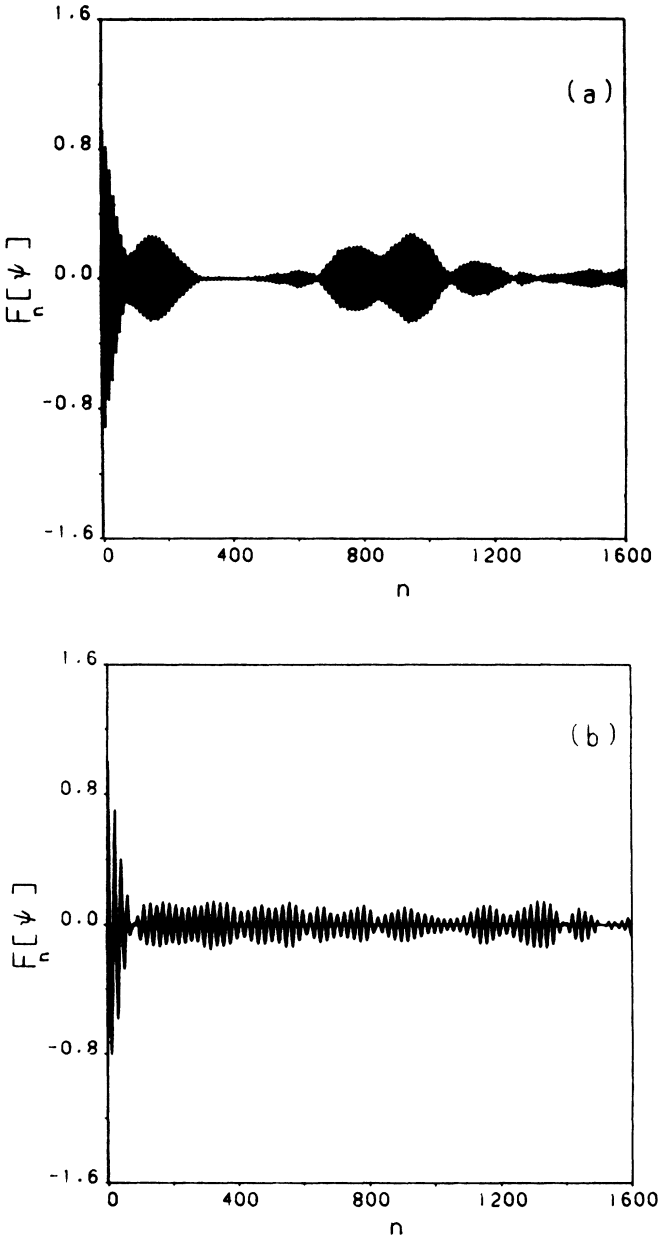

FIG. 12. Same as in Fig. 10 for the localized eigenfunction at $k=64.1408$. The strong correlation along path 1 confirms the correspondence between regularity and localization.

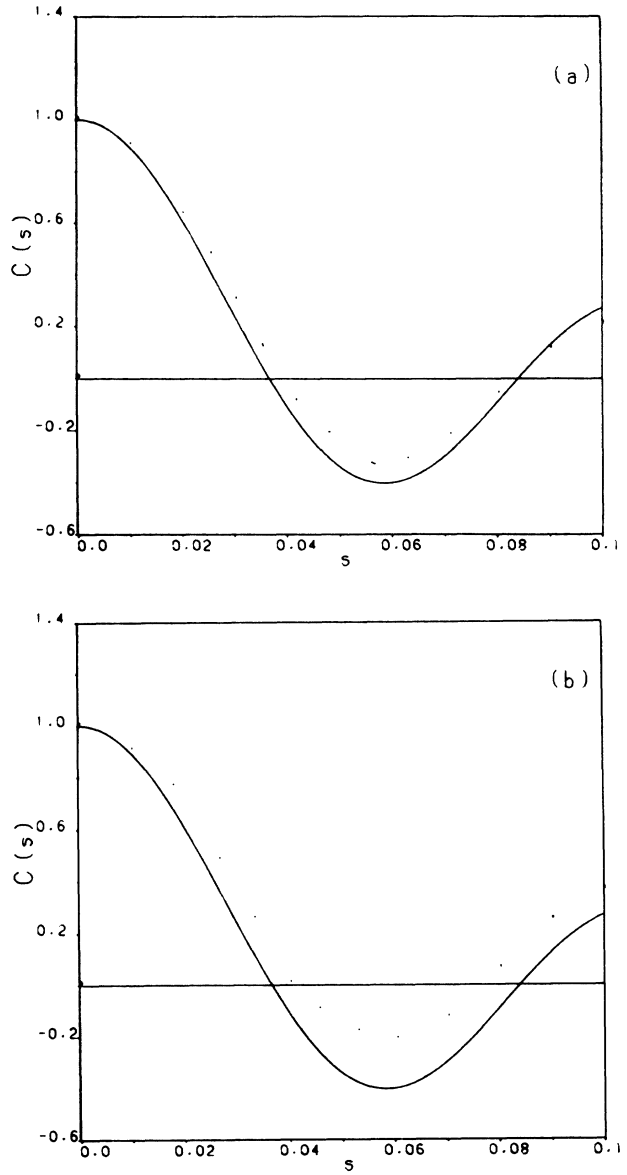

FIG. 13. Globally averaged spatial correlation function $C(\mathbf{s})$ for the (00) mode eigenfunction at $k=65.7698$. The direction of increment ϕ makes an angle of (a) 87° and (b) 171° with the x axis. The continuous curve in both cases is the zeroth-order Bessel function $J_0(ks)$.

retracing periodic orbits (bouncing ball modes as in the stadium) which cover only part of the domain. The choice of coordinates therefore becomes quite simple as indicated in Fig. 16. Following the notation of Bai *et al.*,[24] the x coordinate is taken as the "slow averagable" variable and the transverse y as the "fast parametric" variable. The reason for such a choice is obvious since the smaller amplitude of the y motion is equivalent to a higher frequency. We shall also refer to these as the vibrational and electronic processes, respectively.

The adiabatic Hamiltonian for the y motion parametrized by x can be written as

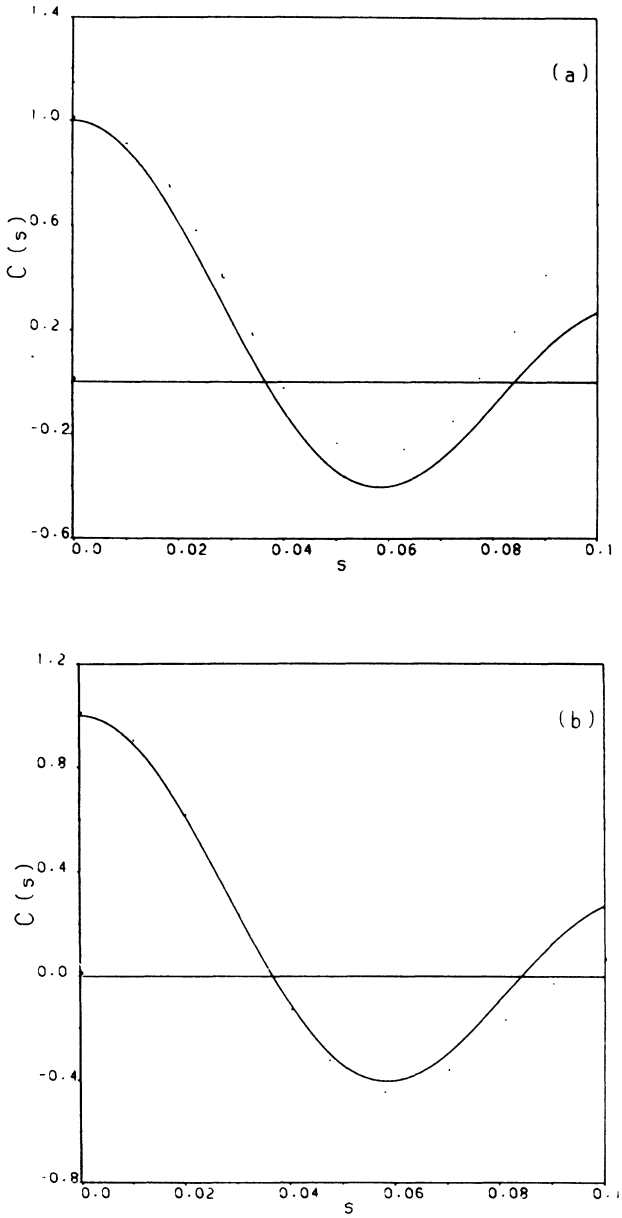

FIG. 14. Same as in Fig. 13 for the (01) parity mode eigenfunction at $k=65.5744$. The deviations from the Bessel function oscillation are considerably larger and the lack of isotropy is more obvious.

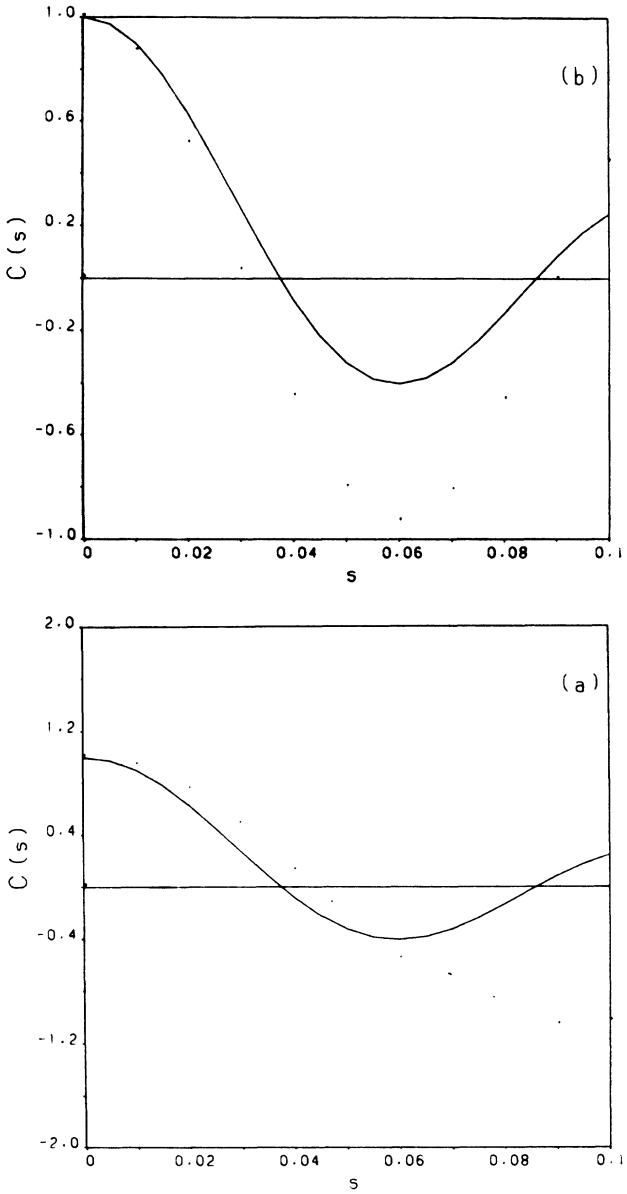

FIG. 15. Spatial correlation function for the localized eigenfunction considered earlier. The angles are the same as in Fig. 13. The oscillations are of a sinusoidal nature.

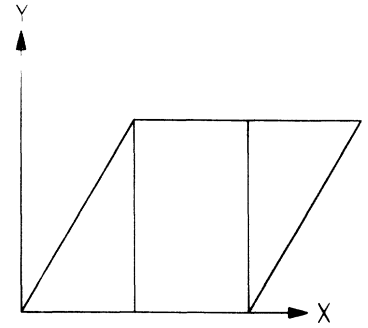

FIG. 16. Coordinates along which the adiabatic separation is carried out. The existence of the bouncing ball modes makes the choice quite obvious.

$$H_y(x)=\frac{-d^2}{d_y^2}+V(y;x)\ , \tag{4.1}$$

where

$$V(y;x)=\begin{cases}\infty, & y<y_1(x)\\ 0, & y_1(x)<y<y_2(x)\\ \infty, & y>y_2(x)\end{cases} \tag{4.2}$$

$$y_1x=\begin{cases}0, & 0<x<L\\ \sqrt{3}(x-L), & L<x<3L/2\end{cases} \tag{4.3}$$

$$y_2(x)=\begin{cases}\sqrt{3}x, & 0<x<L/2\\ \sqrt{3}L/2, & L/2<x<3L/2.\end{cases} \tag{4.4}$$

The corresponding Schrödinger equation now has the form

$$H_y(x)\phi_n(y;x)=E^n(x)\phi_n(y;x)\ , \tag{4.5}$$

where $\phi_n(y;x)$ and $E^n(x)$ are the eigenfunctions and eigenvalues, respectively. Clearly, the solution has to be expressed in two parts. For $0<x<L$

$$\phi_n(y;x)=A_n\sin[n\pi y/y_2(x)] \tag{4.6a}$$

and for $L<x<3L/2$

$$\phi_n(y;x)=A_n\sin[n\pi(\sqrt{3}L/2-y)]/[\sqrt{3}L/2-y_1(x)]\ . \tag{4.6b}$$

The eigenvalues are

$$E^n(x)=\begin{cases}n^2\pi^2/y_2^2(x), & 0<x<L\\ n^2\pi^2/[\sqrt{3}L/2-y_1(x)]^2, & L<x<3L/2.\end{cases} \tag{4.7a}$$

(4.7b)

As yet we have merely found the eigensolutions of a particle in a one-dimensional box of length $y_2(x)-y_1(x)$. Writing the total adiabatic wave function as

$$\xi^A_{nm}(x,y)=\phi_n(y;x)\zeta(x)\ , \tag{4.8}$$

the Hamiltonian for the x motion turns out to be

$$H_n=\frac{d^2}{d_x^2}+E^n(x)\ , \tag{4.9}$$

and the corresponding Schrödinger equation is

$$H_n\zeta_m(x)=E^A_{nm}\zeta(x)\ , \tag{4.10}$$

where E^A is the total adiabatic energy of the state labeled by n and m.

The interesting feature that this approximation brings about is that the potential for the x motion is just the energy for the y motion. To proceed with our analysis on localized states, we must consider the shape of the potential $E^n(x)$ given by Eq. (4.7). The potential is constant over the region $L/2<x<L$ and varies as n^2/x^2 and $n^2/(3L/2-x)^2$ over $0<x<L/2$ and $L<x<3L/2$, respectively. The steepness of the walls in the triangular region increase rapidly with n. Obviously, therefore, the adiabatic wave functions for large electronic (n) and low vibrational (m) states would remain confined to the rectangular region.

Coming back to the exact problem, if one were to expand the eigenfunction in terms of the adiabatic states

$$\psi(x,y)=\sum_i c_i\xi_i(x,y)\ , \tag{4.11}$$

the coefficient c_i would be nearly 1 for those exact and adiabatic states for which the overlap (ξ_i,ψ) is large. This would be so, in particular, for all eigenfunctions ψ which are localized to the rectangular domain since the separation involves no approximation in this region. One would therefore expect the exact problem to have a large number of regular eigensolutions, each having an eigenvalue and an eigenfunction close to that of a single adiabatic state. These would naturally persist even at higher energies. Since an identical analysis holds for both the bands shown in Fig. 6, the wave function would be a superposition of the two.

In Table V, we compare the exact eigenvalues obtained numerically with those of a particle confined to a rectangular box with sides $\sqrt{3}L/2$ and $L/2$ and labeled by the integers n and m. For reasons mentioned above, we have investigated only those cases where $m\leq 4$.

At very low energies, the exact and the rectangular eigenvalues match to within 4%. The eigenfunctions are found to be localized, but not strictly over the two bands (Fig. 1). As the shape of potential suggests, the adiabatic wave function $\xi^A_{n,1}$ for small n takes nonzero values well into the triangular regions (Fig. 8). Thus regularity in this case is probably due to a weak mixing of adiabatic states.

At intermediate energies, the eigenvalues (exact and rectangular) match to within 0.1% and the eigenfunctions are sharply localized over the rectangular region. At higher energies, the agreement gets better, as expected.

TABLE V. Comparison of the (00) parity mode eigenvalues obtained numerically with those of a rectangular box over a wide range of energy. The corresponding eigenfunctions were found to be regular.

k_{00} (exact)	n	m	k (rectangular)
8.9611	5	1	9.1651
26.1177	15	1	26.1534
26.8124	15	2	26.6646
51.9651	30	1	52.0481
52.2709	30	2	52.3067
52.7289	30	3	52.7552
64.1408	37	1	64.1561
64.3788	37	2	64.3661
64.6990	37	3	64.7148
78.0142	45	1	78.0000
78.1591	45	2	78.1729
78.4560	45	3	78.4601
83.9309	49	1	83.9235
84.0741	49	2	84.0823
84.4101	49	3	84.3464
84.7413	49	4	85.7146

V. SPECTRAL STATISTICS—EXPLANATIONS

In the following, we seek to explain our results on the spectral fluctuations discussed in Sec. II. As mentioned earlier, the particular values of ν and $\bar{\nu}$ do not fit in with the classical description of the system. It would therefore seem that there is little justification in using Eqs. (2.5) and (2.11) for describing the nearest-neighbor spacing distribution and the spectral rigidity, respectively. However, a crucial ingredient in the derivation of these results is the assumption that the level densities ρ_i $(i=1,2)$ of the regular (Poisson) and the irregular (GOE distributed) part of the spectrum are proportional to the Liouville measures of the regular and chaotic regions, respectively. Implicit here is also the assumption that eigenvalue sequences obey GOE statistic only if the corresponding classical system is choatic.

Our studies on the properties of the (00) parity mode eigenfunctions reveal the simultaneous occurrence of both regular and irregular states. In the former case, the eigenfunctions are localized on the rectangular bands shown in Fig. 6 and are nearly zero in the rest of the domain. The Born-Oppenheimer approximation offers a suitable explanation for their existence and allows them to be labeled by quantum numbers m and n. Thus there exists a sequence of levels corresponding to the irregular eigenfunctions and a regular sequence characterized by two quantum numbers. We perform a simple calculation to show that the quantities ν and $\bar{\nu}$ are, in fact, proportional to the fraction of regular and irregular states in the system.

Let the number of regular states (localized on the two bands or arising from a weak mixing of the adiabatic states) corresponding to each electronic state (n) be equal to $\alpha(n)$. Assuming the eigenvalues to be those of a rectangular box, the number of regular states having an energy less than E is thus

$$\begin{aligned} N^R(E) &= n\alpha(n) \\ &= [k^2/3 - 3\alpha^2(k)]^{1/2}\alpha(k) \\ &\approx k\alpha(k)/\sqrt{3} \ . \end{aligned} \tag{5.1}$$

Since the explicit form of $\alpha(k)$ is not known, let α_A be the mean in the interval $25<k<70$. The number of regular states in this interval would then be $N^R(k)=k\alpha_A/\sqrt{3}$. The total number of states in this interval is easily found using the corrected Weyl formula

$$N(k) = Ak^2/4\pi + (L_N - L_D)k/4\pi + C \ , \tag{5.2}$$

where A is the area of the domain, L_N and L_D are the lengths of the Neumann and Dirichlet edges, respectively, and C is a correction due to the vertex. Thus the fraction of regular states $N^R(k)/N(k)$ in the interval $25<k<70$ is equal to $0.08\alpha_A$. On equating this to the value of ν obtained from the best fit to the spacing distribution, α_A turns out to be ≈ 2.5. Thus the mean number of regular states corresponding to each electronic state is 2.5—a result that is quite reasonable, as we see from Table V.

VI. CONCLUDING REMARKS

We have numerically investigated various statistical properties of the eigenvalue spectrum and eigenfunctions of the quantum $\pi/3$-rhombus billiard with a view towards understanding the manifestations of nonintegrability in this simple pseudointegrable system. Our results can be summarized as follows.

(i) The spectral statistics of the pure rhombus modes results from an independent superposition of a sequence of GOE distributed levels with relative weight $\bar{\nu}=0.8$ and a Poisson sequence with relative weight $\nu=0.2$. In order to distinguish between the quantities obtained by studying the classical motion and the best fit to the spacing distribution, we refer to these as $\bar{\nu}_{\rm cl}$ and $\bar{\nu}_{\rm qm}$. In the present case $\bar{\nu}_{\rm cl}=0$ while $\bar{\nu}_{\rm qm}=0.8$. A drastic change in the difference seems unlikely at higher energies. Hence chaotic dynamics, characterized by an exponential divergence of trajectories, is not a necessary condition for a GOE-like spectrum.

(ii) *Most* eigenfunctions of the pure rhombus modes are irregular, though the underlying classical dynamics is at best confined to a double torus. The spatial correlation function is anisotropic and shows considerable deviation from the Bessel function oscillations, thereby indicating that diffraction from vertices does not play an important role.

(iii) Regular states do exist at all energies in the (00) parity mode of the $\pi/3$-rhombus billiard. Barring those at low energy, the rest are predominantly localized on the two bands shown in Fig. 6. Their statistical properties are similar to those of the equilateral triangle eigenfunctions.

(iv) The BOA explains the presence of these in terms of a confining mechanism arising from a dynamical potential. The eigenvalues (exact and adiabatic) are in good agreement, especially at higher energies. Regularity at lower energies is probably due to a weak mixing of adiabatic states.

(v) The presence of regular states affects the spectral fluctuations. Based on the results of Secs. II and V, it is shown that the quantities ν and $\bar{\nu}$ in the Berry-Robnik formula are in fact the fraction of regular and irregular states in the corresponding quantum system. The results should hold for all generic polygonal billiards since these have zero Kolmogorov entropy.

(vi) Hence it is proposed that a sequence of eigenvalues corresponding to irregular quantum states give rise to GOE statistics.

ACKNOWLEDGMENTS

It is a great pleasure to thank Professor S.V. Lawande and Professor M.V. Berry for stimulating discussions.

APPENDIX

The results of Secs. II and III are based on the boundary-dipole-distribution technique developed[7] and demonstrated[8] by Riddell. Since it has already been discussed by McDonald in detail,[5] we shall only briefly touch upon it.

A solution of the Helmholtz equation

$$(\nabla^2+k_n^2)\psi_n(\mathbf{r})=0\ , \tag{A1}$$

$\psi_n(\mathbf{s})=0$ ($\mathbf{s}\in\mathbb{R}$), in a two-dimensional interior domain R can be expressed in terms of a dipole distribution $D(\mathbf{s})$ on the boundary. One can write

$$\psi(\mathbf{r})=\oint_{\partial R} D(\mathbf{s}')[\nabla' G(\mathbf{r},\mathbf{s}')]\cdot d\mathbf{s}'\ , \tag{A2}$$

where $\mathbf{r}\in\mathbb{R}$, $\mathbf{s}'\in\mathbb{R}$, and $G(\mathbf{r},\mathbf{s}')$ is the free-space Green's function for the Helmholtz equation. In two dimensions,

$$G(\mathbf{r},\mathbf{s}')=-\frac{i}{4}H_0^{(1)}(k_n|\mathbf{r}-\mathbf{s}'|)\ , \tag{A3}$$

where $H_0^{(1)}$ is the Hankel function of the first kind. Thus

$$\psi_n(\mathbf{r})=\frac{ik_n}{4}\oint_{\partial R} D(\mathbf{s}')H_1^{(1)}(k_n|\mathbf{s}'-\mathbf{r}|)\frac{(\mathbf{s}'-\mathbf{r})}{|\mathbf{s}'-\mathbf{r}|}\cdot\hat{\mathbf{n}}(\mathbf{s}')ds'\ , \tag{A4}$$

where $n(\mathbf{s}')$ is the outward normal to the boundary at $\mathbf{s}'$. In a bounded region such as R, the complex Hankel function $H_1^{(1)}$ can be replaced by the real Neumann function N_1 (more specifically, $iH_1^{(1)}\rightarrow -N_1$). Thus

$$\psi_n(\mathbf{r})=\frac{k_n}{4}\oint_{\partial R} D(\mathbf{s}')\frac{(\mathbf{s}'-\mathbf{r})}{|\mathbf{s}'-\mathbf{r}|}\cdot\hat{\mathbf{n}}(\mathbf{s}')K(\mathbf{s},\mathbf{s}';k_n)ds'=0\ , \tag{A5}$$

where $K(\mathbf{r},\mathbf{s}';k_n)=N_1(k_n|\mathbf{s}'-\mathbf{r}|)$.

One obtains the boundary integral equation by taking the limit as $\mathbf{r}$ approaches the boundary from within. Since ψ is zero on the boundary, the dipole distribution satisfies

$$D(\mathbf{s})-\frac{k_n}{2}\oint_{\partial R} D(\mathbf{s})\frac{(\mathbf{s}'-\mathbf{s})}{|\mathbf{s}'-\mathbf{s}|}\cdot\hat{\mathbf{n}}(\mathbf{s}')K(\mathbf{s},\mathbf{s}';k_n)ds'=0\ . \tag{A6}$$

An advantage of replacing $H_1^{(1)}$ by N_1 is that for computational purposes the number of unknowns is halved. However, there is a disadvantage as well. While the Helmholtz equation has no eigenvalue if the solution satisfies an outgoing boundary condition (Sommerfeld radiation condition) at infinity, it does have eigensolutions if the choice of iN_1 rather than $H_1^{(1)}$ is made. As a result, one obtains eigenvalues of the exterior problem as well. To circumvent this difficulty the kernel function is taken to be

$$K(\mathbf{s},\mathbf{s}';k_n)=N_1(k_n|\mathbf{s}'-\mathbf{s}|)+\alpha J_1(k_n|\mathbf{s}'-\mathbf{s}|)\ , \tag{A7}$$

where α is a real coefficient of the Bessel function J_1. This does not disturb the physical results of the interior problem, but the eigenvalues of the exterior (Neumann) problem start depending on α.

The eigenvalues can now be computed by discretizing Eq. (A6). We have worked with a maximum of 100 boundary points on the first quadrant only, since others can be obtained by reflections about the two diagonals. This also helps us to separate the four symmetry modes mentioned in Sec. II. In general, it is sufficient to have the number of boundary points $N=k+20$, where $k^2=2mE/\hbar^2$. The eigenfunctions can similarly be computed from Eq. (A5) by obtaining the dipole distribution at a desired eigenvalue.

Finally, we mention the distinct advantages that this method offers. First, it requires points only on the boundary for the construction of eigenfunction. Second, any region of the spectrum can be independently investigated without compromising the accuracy. In fact, the accuracy depends only on the choice of N and not on the number of solutions possible.

[1]B. Eckhardt, Phys. Rep. **163**, 205 (1988).
[2]M. V. Berry, Ann. Phys. (N.Y.) **131**, 163 (1981).
[3]M. C. Gutzwiller, J. Math. Phys. **8**, 1979 (1967); **10**, 1004 (1969); **11**, 1791 (1970); **12**, 343 (1971).
[4]M. C. Gutzwiller, Physica D **5**, 183 (1982).
[5]S. W. McDonald, Ph.D. thesis (University Microfilms Report No. 8413506, Ann Arbor, MI, 1983).
[6]S. W. McDonald and A. N. Kaufman, Phys. Rev. A **37**, 3067 (1988).
[7]R. J. Riddell, Jr., J. Comput. Phys. **31**, 21 (1979).
[8]R. J. Riddell, Jr., J. Comput. Phys. **31**, 42 (1979).
[9]D. Wintgen, Phys. Rev. Lett. **61**, 1803 (1988).
[10]R. Aurich and F. Steiner, Physica D **32**, 451 (1988).
[11]R. Aurich and F. Steiner, Physica D **39**, 169 (1989).
[12]R. Aurich and F. Steiner, Physica D (to be published).
[13]M. V. Berry and M. Tabor, Proc. R. Soc. London. Ser. A **356**, 375 (1977).
[14]O. Bohigas, M. J. Giannoni, and C. Schmit, Phys. Rev. Lett. **52**, 1 (1984).
[15]M. V. Berry, Proc. R. Soc. London Ser. A **400**, 229 (1985).
[16]T. H. Seligman, J. J. M. Verbaarschot, and M. R. Zirnbaur, Phys. Rev. Lett. **53**, 215 (1984).
[17]T. Ishikawa and T. Yukawa, Phys. Rev. Lett. **54**, 1617 (1985).
[18]E. Haller, H. Koppel, and L. S. Cederbaum, Phys. Rev. Lett. **52**, 1665 (1984).
[19]M. V. Berry and M. Robnik, J. Phys. A **17**, 2413 (1984).
[20]Th. Zimmermann, H. D. Meyer, H. Koppel, and L. S. Cederbaum, Phys. Rev. A **33**, 4334 (1986).
[21]H. D. Meyer, E. Haller, H. Koppel, and L. S. Cederbaum, J. Phys. A **17**, 1831 (1984).
[22]M. Shapiro, D. D. Taylor, and P. Brumer, Chem. Phys. Lett. **106**, 325 (1984).
[23]R. D. Taylor and P. Brumer, Faraday Discuss. Chem. Soc. **75**, 117 (1983).
[24]Y. Y. Bai, G. Hose, K. Stefanski, and H. S. Taylor, Phys. Rev. A **31**, 2821 (1985).
[25]E. J. Heller, Phys. Rev. Lett. **53**, 1515 (1984); in *Quantum Chaos and Statistical Nuclear Physics*, Vol. 263 of *Lecture Notes in Physics*, edited by T. H. Seligman and H. Nishioka (Springer-Verlag, Berlin, 1986).

[26]E. B. Bogomolny, Physica D **31**, 169 (1988).
[27]M. V. Berry, Proc. R. Soc. London Ser. A **423**, 219 (1989).
[28]A. N. Zemlyakov and A. Katok, Mat. Zametki **18**, 291 (1975) [Math. Notes **18**, 760 (1976)].
[29]P. J. Richens and M. V. Berry, Physica D **2**, 495 (1981).
[30]T. Cheon and T. D. Cohen, Phys. Rev. Lett. **62**, 2769 (1989).
[31]P. Seba, Phys. Rev. Lett. **64**, 1855 (1990).
[32]B. Eckhardt, J. Ford, and F. Vivaldi, Physica D **13**, 339 (1984).
[33]J. B. Keller and S. I. Rubinow, Ann. Phys. (N.Y.) **9**, 24 (1960).
[34]M. Gaudin, J. Phys. (Paris) **48**, 1633 (1987).
[35]T. H. Seligman and J. J. M. Verbaarschot, Phys. Lett. **108A**, 183 (1985).
[36]H. P. Baltes and E. R. Hilf, *Spectra of Finite Systems* (Wissenchaftsverlag, Mannheim, 1976).
[37]A. Shudo, Prog. Theor. Phys. Suppl. **98**, 173 (1989).
[38]F. J. Dyson and M. L. Mehta, J. Math. Phys. **4**, 701 (1963).
[39]T. H. Seligman, and J. J. M. Verbaarschot, J. Phys. A **18**, 2227 (1985).
[40]P. Pechukas, J. Chem. Phys. **57**, 5577 (1972).
[41]N. DeLeon and E. J. Heller, Phys. Rev. A **30**, 5 (1984).
[42]M. Shapiro and G. Goelman, Phys. Rev. Lett. **53**, 1714 (1984).
[43]M. V. Berry, J. Phys. A **10**, 2083 (1977).
[44]K. Stefanski and H. S. Taylor, Phys. Rev. A **31**, 2810 (1985).